JOURNAL OF MATERIALS SCIENCE 19 (1984) 3166–3172

Theoretical analysis of the deflection test used in single-surface oxidation of metallic samples

J. G. ZHAO, A. M. HUNTZ
Laboratoire de Métallurgie Physique, LA no. 177, Université Paris-Sud, 91405 Orsay Cédex, France

On the basis of the experimental results on deflection obtained by Delaunay during single-surface oxidation of metallic samples, a theoretical analysis of this deflection test was carried out. Two important problems were established concerning the physical signification of the oxide stress calculated from the measured deflection and the relation between the oxide adherence and the oxide stress. In particular, it appears that the oxide stress level determined by the deflection test is only representative of the stresses relieved by the sample curvature. Secondly, spalling of the oxide layer is directly related to the product of the residual stress value by the curvature of the sample. Some experimental results, recently obtained, confirm this theoretical analysis.

1. Introduction

Spalling of oxide scales is a disastrous phenomenon in the protection from corrosion of metallic materials and the mechanisms of adherence loss are virtually unknown in most cases [1]. Therefore, it is necessary to draw attention to the study of adherence phenomena. Oxide scales developed on metallic substrates by oxidation can be destroyed during either isothermal oxidation or cooling. The internal stresses are considered to be the chief cause of oxide spalling. The limited amount of experimental apparatus [2, 3] allowing the measurement of the internal stresses of oxide scales, explains why few studies have been done, to date, in order to pinpoint spalling mechanisms. One method mainly used for stress measurement (X-ray diffraction [4, 5]), cannot yield information on stresses developed during isothermal oxidation at high temperature, but only on residual stresses in the oxide scale after cooling. Other methods, based on numerical calculation, such as the deflection test on thin samples selectively oxidized on one face [2, 3, 6, 7] only allow qualitative and comparative studies. In order to extend the possibilities of such techniques, many theoretical studies must be undertaken: it is essential to determine the physical meaning of the stress calculated from the deflection values and to pinpoint deformation processes and the relationship to oxide scale adherence. In this paper, on the basis of experimental results obtained by Delaunay and Norin [2, 3, 6, 7] we attempt a theoretical analysis of the deflection test in single-surface oxidation (the so-called DTMO) and to confirm this analysis by some new experimental results.

2. Theoretical analysis

2.1. Physical meaning of the stress calculated from deflection tests

The experimental system used in DTMO is first examined. The examined sample (45 mm × 5 mm × 0.15 mm) (Fig. 1) is first covered on one face by a thin SiO_2 layer (~ 500 nm thick) which protects it from further oxidation. Another face is then polished and the specimen submitted to oxidation. When oxidation is taking place, oxide scale grows on the unprotected face and stresses are partially relieved by the curvature of the duplex sample, metallic substrate and oxide scale. The apparatus described by Delaunay *et al.* [2, 3] allows the measurement of deflection, D.

Assuming that the SiO_2 protective layer has

0022–2461/84 $03.00 + .12

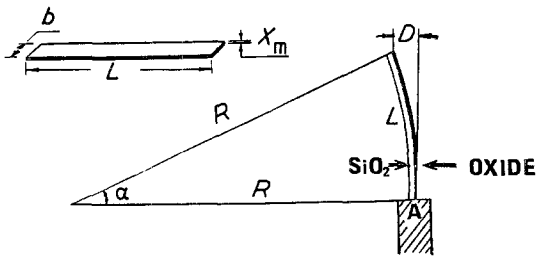

Figure 1 Specimen used in the deflection test.

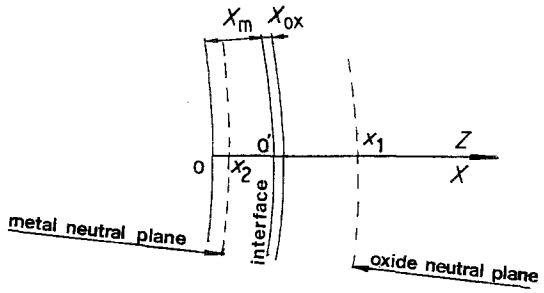

Figure 2 Imaginary system.

no effect on the system, the sample can be considered to be a two-part specimen and, on account of the differences in physical properties and of the possibilities of coherence relations between the two parts, such specimens can bend towards either the SiO_2 or the oxide layer. For given values of P_{O_2}, T, t, L (metallic sample length), X_m (metallic sample thickness), X_{ox} (oxide thickness), a value of the deflection, D, is determined.

In order to determine the nature and physical meaning of the stress which induces the deflection, we considered an imaginary system consisting of two layers whose dimensions are, respectively, $L \times b \times X_m$ and $L \times b \times X_{ox}$, and which is similar to the experimental system. Imaginary stresses $\sigma_{m(x)}$ and $\sigma_{ox(z)}$ are, respectively, applied to the metallic substrate and to the oxide layer in order to bend this imaginary specimen (Figs. 2 and 3) under the same conditions operating for the experimental sample. The values of these stresses may be calculated by the infinite elements method. With the assumption that the specimen bends by elastic deformation ($\sigma = E\epsilon$), the stress values are given by*:

$$\sigma_{ox} = -E\frac{X_m^2}{3L^2}\frac{D}{X_{ox}}$$

and

$$\sigma_m = E\frac{2D}{3L^2}(x - \tfrac{1}{3}X_m)$$

In the case of plastic deformation, by writing Holloman's law $\sigma = k\epsilon^r$, then†:

$$\sigma_{ox} = -k_m\left(\frac{2D}{L^2}\right)^r \frac{X_m^{r+1}}{(r+1)(r+2)X_{ox}}$$

$$\sigma_m = k_m\left(\frac{2D}{L^2}\right)^r \left(x - \frac{X_m}{r+2}\right)^r$$

where k_m and r are the consolidation coefficients of the metallic substrate. These values of σ_{ox} and σ_m correspond to the stresses applied to the imaginary system in order to bend it under the same conditions as the true specimen. However, the experimental specimen is not submitted to external stresses. Therefore, what is the correspondence of the additional stress in the true system? It is necessary to consume energy in order to bend the imaginary system while the true sample bends itself. Thus, we can say that the imaginary system consumes external stress and the true specimen internal stress. Thus, the measured deflection is a manifestation of oxide–substrate internal stresses. By the empirical Norin's formula:

$$\sigma_{ox} = \frac{E}{1-\nu^2}\frac{X_m^2}{3L^2}\frac{D}{X_{ox}}$$

it was possible to calculate σ_{ox}, when D and X_{ox} were determined. This stress value, so calculated, is only relative to a part of the internal stresses (or an amount of internal energy) which is relieved by the curvature of the specimen. We term this accommodated stress, σ_a. The value of σ_a does not represent the total internal stress. In the specimen, other stresses can be relieved by other methods, such as recrystallization, and it subsists a residual internal stress which we term σ_r.

Thus, with the assumption that all internal stresses proceed from oxidation (no other source of internal stress), we can say that σ_a, measured by DTMO, is a part of the internal stress created by oxidation. In addition, with the assumption that there is no other phenomenon able to relieve the internal stresses, we can write:

$$\sigma_t = \sigma_a + \sigma_r$$

where σ_t is the total internal stress.

*See Appendix I.
†See Appendix II.

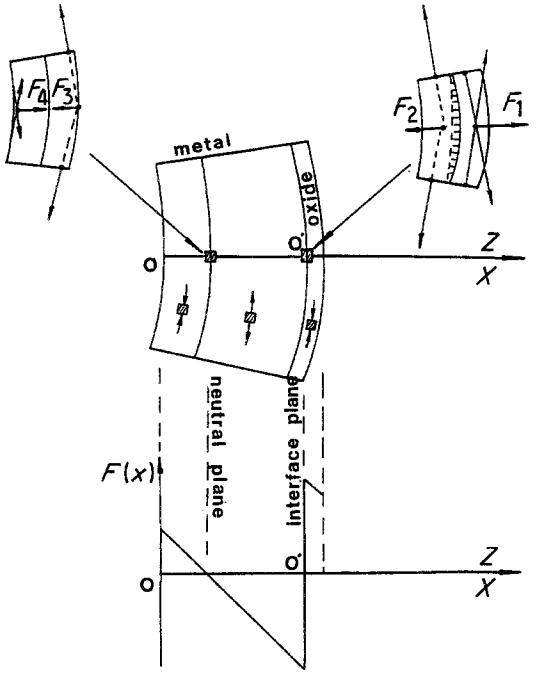

Figure 3 Schematic illustration of the strength distribution ($F(x)$) along the arbitrary axis.

2.2. Relation between oxide scale spalling and σ_a

If we examine Fig. 3, it can be seen that the oxide scale spalling is caused by the $F(x)$ strength applied at the oxide–substrate interface. By using the formula $\sigma_t = \sigma_r + \sigma_a$, the greater the σ_a value, the smaller the σ_r value for a given oxide thickness X_{ox}, and so the smaller the $F(x)$ value. But, with Norin's formula, the greater the σ_a value, the greater the D/X_{ox} or $d\alpha/dL$ values, and so the greater the $F(x)$ value for a given X_{ox} value (Fig. 4). By considering that $d\alpha/dL$ increases slowly while σ_r decreases rapidly when σ_a increases, we can conclude that the experimental σ_{max} peak observed (Fig. 4a) does not correspond to a σ value for which the oxide scale will be damaged by spalling. Oxide scale spalling will appear at a high value of σ_r, i.e. when $\sigma_a \sim \sigma_{int.}$ or when X_{ox} is higher than a given value which is not easy to determine. From a theoretical point of view, oxide scale spalling is related to the product $\sigma_r(d\alpha/dL)$.

Our theoretical analysis allows one to understand the physical meaning of σ calculated by Norin's formula from DTOM and, consequently, to resolve the difficult interpretation of the σ_{max} peak observed by Delaunay and Norin for a small oxide scale thickness. This σ_{max} value only indicates that for a small oxide thickness, most of the stresses are relieved by deflection. Spalling will occur much later, when σ_r and $d\alpha/dL$ will be important.

3. Confirmation of analysis by experimental results

In order to confirm this analysis, we have carried out some experimental deflection tests on the same apparatus as Delaunay [2, 3] using two different alloys: $FeCr_{23}Al_5$ and a $Ni_{76}Cr_{16}Fe_8$ (Inconel 600), alloys which, respectively, develop

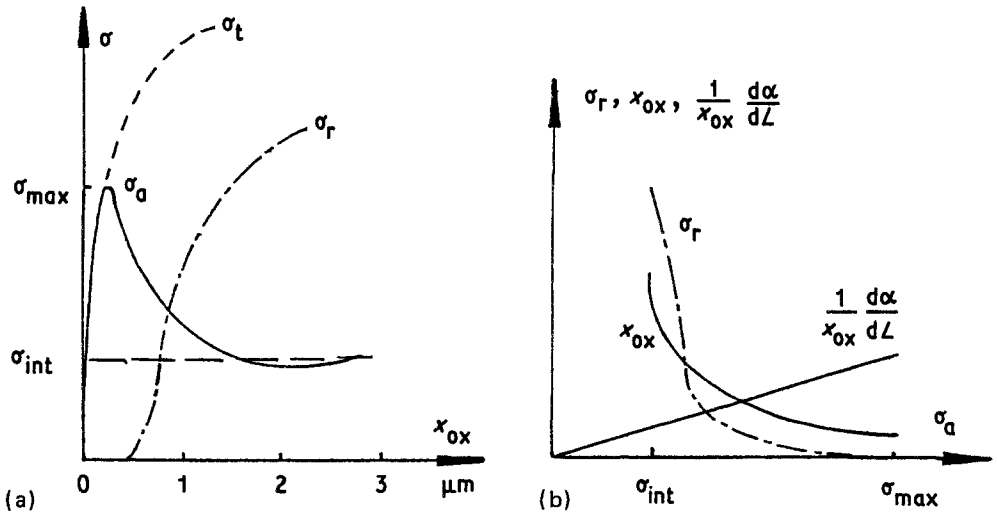

Figure 4 (a) Curve of $\sigma = f(X_{ox})$: σ_a is obtained from the results of Delaunay *et al.* [2, 3], σ_r is a theoretical curve and σ_t the curves due to $\sigma_a + \sigma_r$. (b) Curves of σ_r or X_{ox} or $(1/X_{ox})(d\alpha/dL) = f(\sigma_a)$; the first is a theoretical curve while the others are taken from Delaunay's results and Norin's formula [2, 3, 6, 7].

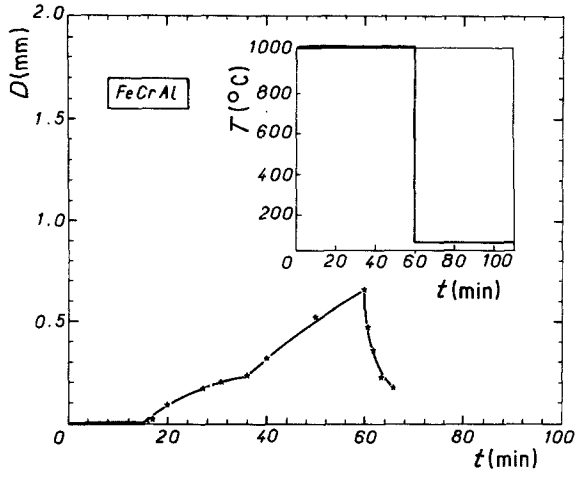

Figure 5 Curve of $D = f(t)$ obtained for a $FeCr_{23}Al_5$ sample (pre-treated at 1000° C), then protected on one face by a SiO_2 layer and submitted to the deflection test for 1 h at 1000° C under pure O_2.

by oxidation an inner protective scale of Al_2O_3 and Cr_2O_3 [8–10]. Our results are shown in Figs. 5 to 9. For the FeCrAl alloy, we observed that the relieved stress, σ_a,* is a linear function of X_{ox} (Fig. 7), with a high slope, during isothermal oxidation. This shape is related to the fact that the specimen deflection begins only when oxidation kinetics have reached a steady state due to alumina growth (A on Fig. 6). While the total internal stresses are created simultaneously by oxidation, the manifestation of σ_a, i.e. the stress accommodation by the sample curvature, only appears after some oxidation time. This phenomenon shows that the stress calculated from DTOM is only a part of the total stress created by oxidation.

For the NiCrFe alloy, the deflection test does not induce sample curvature during isothermal oxidation at 1000° C (Fig. 8), but an important value of D is recorded during slow cooling. This deflection is a linear function of the temperature decrease. By assuming that the internal oxide stresses during cooling are related to the difference of contraction coefficients of the oxide and the metallic substrate, we developed a formula which allows one to calculate D during cooling (see Appendix III):

$$D = \left[(\alpha_m - \alpha_{ox}) \Big/ \frac{X_m}{3L^2}\left(4 + \frac{E}{E_{ox}}\frac{X_m}{X_{ox}}\right)\right](T_0 - T)$$

where T_0 is the isothermal oxidation temperature, T the temperature at time t, α_m, α_{ox}, the metallic and oxide linear expansion coefficients, respectively, E, E_{ox}, Young's modulus of the metal and oxide, respectively, and X_m, X_{ox}, the thickness of the metal and the oxide, respectively.

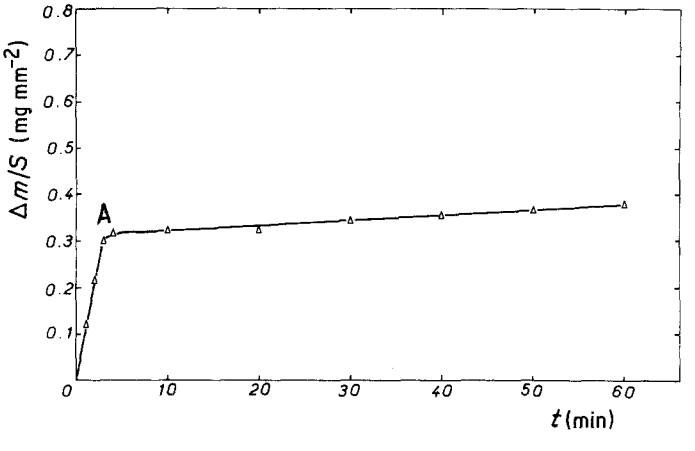

Figure 6 Thermogravimetric curve obtained on FeCrAl sample oxidized in the same conditions as for DTMO (Fig. 5).

*σ_a curve is obtained by using the Norin formula and the experimental results of deflection (Fig. 5) and of thermogravimetry (Fig. 6).

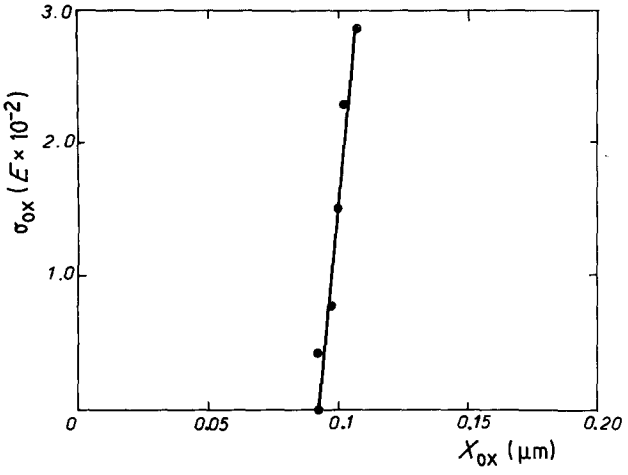

Figure 7 Curve of $\sigma_{ox} = f(X_{ox})$ obtained from curves of Figs. 5 and 6, for a FeCrAl sample oxidized on one face at 1000° C. E, the Young's modulus of the alloy at the oxidation temperature, has the same unit as σ_{ox}.

There is a good agreement between this formula and the results obtained with the Inconel 600 (Fig. 9). Nevertheless, the theoretical estimation of the slope of the curve $D = f(T_0 - T)$ is twice that of the slope of the experimental curve of Fig. 9. This discrepancy confirms our theoretical analysis of DTMO. Sample defection is due to accommodation of a part of stresses σ_a, according to the formula $\sigma_t = \sigma_a + \sigma_r$, and residual stresses subsist in the specimen; this analysis explains the difference between the theoretical and experimental slope of curves $D = f(T_0 - T)$. Moreover, we confirm, by X-ray diffraction, that samples oxidized in conditions of DTMO, then cooled, contained residual stresses. Indeed, oxide of Inconel alloy was found to be submitted to compressive stress at 20° C with a value of $-15.8 \times 10^{-4} E_{ox}$. Again, this result confirms the formula $\sigma_t = \sigma_a + \sigma_r$.

4. Conclusion

A theoretical analysis of DTMO elucidated the physical meaning of the stress calculated on the basis of the deflection test. This oxide internal stress is a part of the total internal stress of the oxide layer, the part which is relieved by the

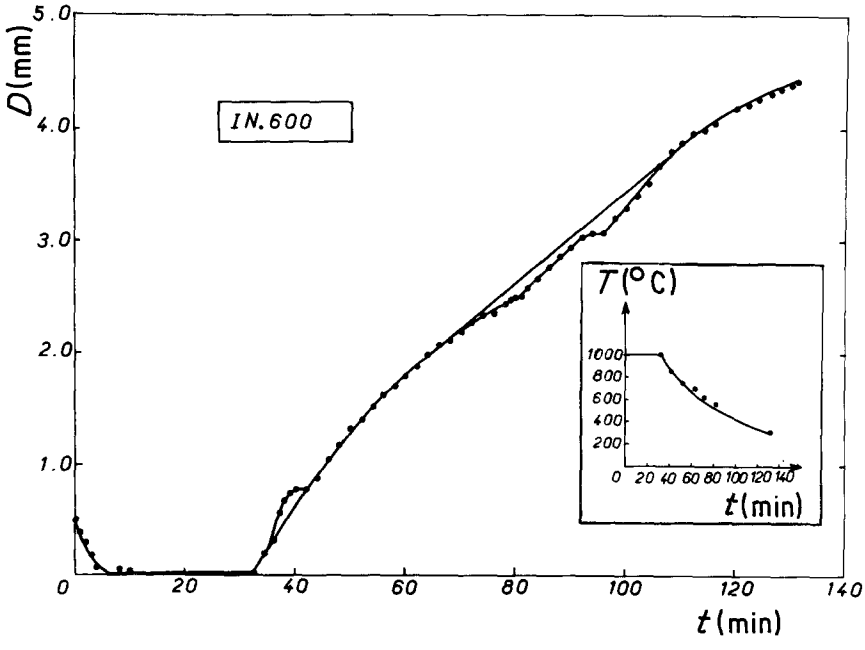

Figure 8 Curve of $D = f(t)$ obtained on a $Ni_{76}Cr_{16}Fe_8$ alloy oxidized for 1 h at 1000°C and cooled under O_2 in the deflection apparatus.

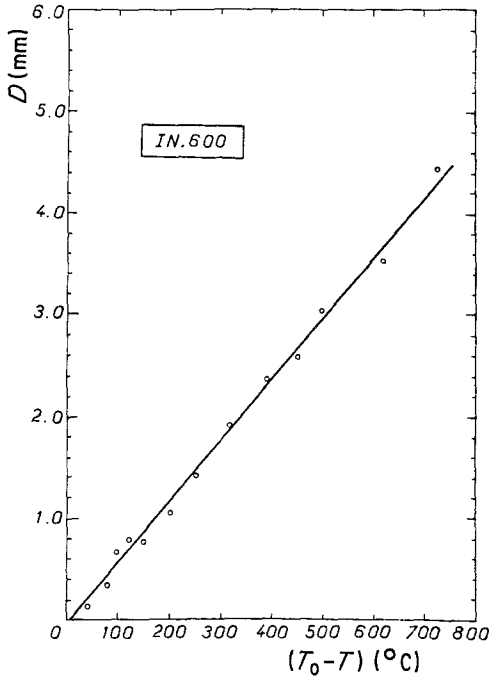

Figure 9 Experimental curve of $D = f(T_0 - T)$ obtained from that part corresponding to the cooling of the curve of Fig. 8 (Inconel alloy).

deflection of the specimen and which we term σ_a. Under such conditions, we can write: $\sigma_t = \sigma_a + \sigma_r$. In addition, the oxide scale spalling is related to the product σ_r $(d\alpha/dL)$. Deflection measured during cooling is directly related to the differences of oxide and metal contraction coefficient and of temperature.

This theoretical analysis allows an interpretation of the experimental results obtained by Norin and Delaunay and is confirmed by our own experimental results.

Appendix I Relation between the deflection D and the oxide and metallic sample stresses in case of elastic deformation

Assumptions:

1. the specimen curvature can be considered as a circle taking into account $D \ll L$;

2. the stresses applied to the imaginary system can be described by:

$$\bar{\bar{\sigma}} = \begin{pmatrix} \sigma & 0 & 0 \\ 0 & 0 & 0 \\ 0 & 0 & 0 \end{pmatrix}$$

since, in this case, $X_m \ll b$ and $b \lesssim L/4$.

Considering that, under equilibrium conditions, the sum of the deflection moments must be equal to zero at point A (Fig. 1) and along the interface plane $(X = X_m,\ z = 0)$ (Fig. 2), and that the sum of the strengths F_1 and F_2 in the direction of the arbitrary axis (Fig. 3) must also be equal to zero, we can write:

$$\begin{cases} \displaystyle\int_0^{X_{ox}}\int_0^{\alpha_m} (\sigma_{ox} b\, dz) \cos\alpha\, d\alpha\, R \sin\alpha \\ \quad + \displaystyle\int_0^{X_m}\int_0^{\alpha_m} (\sigma_m b\, dx) \cos\alpha\, d\alpha\, R \sin\alpha = 0 \\ \displaystyle\int_0^{X_{ox}} \sigma_{ox} b\, dz\, z + \int_0^{X_m} \sigma_m b\, dx (X_m - x) = 0 \\ \displaystyle\int_0^{X_m}\int_0^{\alpha_m} \sigma_m b\, dx\, d\alpha \\ \quad + \displaystyle\int_0^{X_{ox}}\int_0^{\alpha_m} \sigma_{ox} b\, dz\, d\alpha = 0 \end{cases}$$

The first and the third equilibrium equations lead to:

$$\int_0^{X_{ox}} \sigma_{ox} dz + \int_0^{X_m} \sigma_m dx = 0 \qquad \text{(A1)}$$

and the second to:

$$\int_0^{X_{ox}} \sigma_{ox} z dz + \int_0^{X_m} \sigma_m (X_m - x) dx = 0 \qquad \text{(A2)}$$

The expressions for σ_{ox} and σ_m, using Hooke's law and assumption 1, can be written as (cf. Fig. 2):

$$\begin{cases} \sigma_{ox} = E_{ox} \dfrac{2D}{L^2} (z - X_1) & \text{(A3)} \\ \sigma_m = E \dfrac{2D}{L^2} (x - X_2) & \text{(A4)} \end{cases}$$

Solution of these equations gives the values of X_1 and X_2:

$$\begin{cases} X_1 = \dfrac{EX_m^3 + E_{ox}(3X_m X_{ox}^2 - 4X_{ox}^3)}{6E_{ox}(X_m X_{ox} - X_{ox}^2)} \simeq \dfrac{EX_m^2}{6E_{ox}X_{ox}} \\ \qquad + \tfrac{1}{2} X_{ox} \qquad \text{(A5)} \\ X_2 = \dfrac{E_{ox}X_{ox}^3 + E(2X_m^2 - 3X_{ox}X_m^2)}{6E(X_m^2 - X_m X_{ox})} \simeq \tfrac{1}{3} X_m \end{cases}$$

(A6)

Thus in the case of elastic deformation, the stresses needed to bend the imaginary system are given by:

$$\begin{cases} \sigma_{ox}(z) = -\left[E\dfrac{D}{L^2}\dfrac{X_m^2}{3X_{ox}} + E_{ox}\dfrac{D}{L^2}(X_{ox}-2z)\right] & \text{(A7)} \\ \sigma_m(x) = E\dfrac{2D}{3L^2}(x-\tfrac{1}{3}X_m) & \text{(A8)} \end{cases}$$

If we consider that $E \sim E_{ox}$ and $X_{ox} \ll X_m$, the second term may be neglected in Equation A7, then:

$$\sigma_{ox}(z) \simeq \sigma_{ox} = -E\frac{D}{3L^2}\frac{X_m^2}{X_{ox}} \qquad \text{(A9)}$$

Appendix II Relation between D and σ_{ox}, σ_m in the case of plastic deformation

In this case, by applying Holloman's law, $\sigma = k\epsilon^r$, the only difference consists in Equations A3 and A4 which become:

$$\sigma_{ox} = K_{ox}\left(\frac{2D}{L^2}\right)^n (z-X_1)^n \qquad \text{(B1)}$$

$$\sigma_m = K_m\left(\frac{2D}{L^2}\right)^r (x-X_2)^r \qquad \text{(B2)}$$

where n and r are the consolidation coefficients of the oxide and the metallic substrate, respectively.

The solution of Equations A1, A2, B1 and B2 gives the following results, taking into account that $X_{ox} \ll X_m$:

$$\begin{cases} (-X_1)^n \simeq -\dfrac{B}{A}\dfrac{X_m^{r+1}}{(r+1)(r+2)X_{ox}} & \text{(B3)} \\ X_2 \simeq \dfrac{X_m}{r+2} & \text{(B4)} \end{cases}$$

with

$$A = K_{ox}\left(\frac{2D}{L^2}\right)^n$$

and

$$B = K_m\left(\frac{2D}{L^2}\right)^r$$

So, by writing $(z-X_1)^n \simeq (-X_1)^n$ (cf. Fig. 2: $z_{max} = X_{ox} \ll X_1$), we have:

$$\sigma_{ox} = -K_m\left(\frac{2D}{L^2}\right)^r \frac{X_m^{r+1}}{(r+1)(r+2)X_{ox}} \qquad \text{(B5)}$$

$$\sigma_{m(x)} = K_m\left(\frac{2D}{L^2}\right)^r \left(x-\frac{X_m}{r+2}\right)^r \qquad \text{(B6)}$$

Appendix III Relation between the deflection D obtained during cooling and the expansion coefficients α_m and α_{ox}

Assumptions:

1. at the oxidation temperature T_0: $L_{ox} = L_m = L_0$;

2. during cooling, oxidation no longer occurs, or X_{ox} and X_m are considered as constant;

3. the assumptions of Appendix I hold.

Let us consider two foils characterized by an identical initial surface ($L_0 \times b \times X_m$) and ($L_0 \times b \times X_{ox}$), and by their linear expansion coefficients α_m and α_{ox}, respectively; when the temperature decreases from T_0 to T, their lengths will be given by:

$$L_{ox} = L_0[1+\alpha_{ox}(T-T_0)] \qquad \text{(C1)}$$

$$L_m = L_0[1+\alpha_m(T-T_0)] \qquad \text{(C2)}$$

According to the fact that, in case of a good adherence,

$$L_{ox}(1+\epsilon'_{ox}) = L_m(1+\epsilon'_m) \qquad \text{(C3)}$$

where ϵ'_{ox} and ϵ'_m are the values of the foil's deformation at the interface plane. By using Equations A3 to A6 and Hooke's law ($\sigma = E\epsilon$):

$$\epsilon'_{ox} = -\frac{2D}{L^2}\left(\frac{E}{6E_{ox}}\frac{X_m^2}{X_{ox}} + \frac{1}{2}X_{ox}\right) \qquad \text{(C4)}$$

$$\epsilon'_m = \frac{4D}{3L^2}X_m \qquad \text{(C5)}$$

where L is the mean value of L_{ox} and L_m.

The solution of Equations C1 and C5 gives (with $X_{ox} \ll X_m^2/X_{ox}$):

$$D = \left[(\alpha_m-\alpha_{ox})\Big/\frac{X_m}{3L^2}\left(4+\frac{E}{E_{ox}}\frac{X_m}{X_{ox}}\right)\right](T_0-T)$$

References

1. D. P. WHITTLE and J. H. STRINGER, *Phil. Trans. Roy. Soc. London* A295 (1980) 309.
2. D. DELAUNAY, A. M. HUNTZ and P. LACOMBE, *Corros. Sci.* 20 (1980) 1109.
3. D. DELAUNAY, Dr. Ing. thesis, Université Paris XI, Orsay (1980).
4. G. MAEDER, J. L. LEBRUN and J. M. SPRAUEL, *Matériaux et Techniques* 4–5 (1981) 135.
5. G. MAEDER, Conférence aux "Journées d'Extensométrie" organisées par le G.A.M.A.C., Poitiers, September (1981).
6. A. NORIN, final report RMM 1733 Aktibolaget Atomenergie (1969).
7. A. NORIN, *Oxid. Metals* 9 (1975) 259.
8. G. BEN ABDERRAZIK, G. MOULIN, R. BERNERON and A. M. HUNTZ, *J. Mater. Sci.* 19 (1984) 3173.
9. G. MOULIN, *Metaux Corrosion Industrie* (1982) 361; (1983) 1, 81, 121, 201.
10. J. ROUSSELET, G. MOULIN and A. M. HUNTZ, Communication aux Journées de Cinétique Hétérogène, Nancy (1983).

Received 29 September and accepted 11 October 1983